

Muon $g - 2$ in Lepton Portal Dark Matter

Yang Bai^{*} and Joshua Berger[†]

^{*}*Department of Physics, University of Wisconsin-Madison, Madison, WI 53706, USA*

[†]*Department of Physics, Colorado State University, Fort Collins, Colorado 80523, USA*

Abstract

The Lepton Portal Dark Matter model, in which dark matter states only coupling to the charged leptons, can explain the excess of the muon anomalous magnetic moment measured by the Muon $g - 2$ experiment. In this paper, we demonstrate that real, charge-neutral scalar dark matter with a large number of internal degrees of freedom and a mass approximately degenerate with the charged fermionic mediator state can accommodate the $(g - 2)_\mu$ excess. The model remains consistent with the dark matter relic abundance, direct detection, and indirect detection constraints. The dark matter and its charged fermion partner masses are constrained to be below around 200 GeV. The high-luminosity LHC and future lepton colliders, as well as indirect searches at CTA and GAMMA-400, can test this scenario.

1 Introduction

The muon anomalous magnetic moment a key probe of new physics beyond the Standard Model (SM). The latest theoretical calculations have the SM prediction for $a_\mu = (g - 2)_\mu/2$ as [1]

$$a_\mu^{\text{SM}} = 116591810(43) \times 10^{-11} , \quad (1)$$

with the uncertainty dominated by the hadronic vacuum polarization. On the experimental side, the E821 experiment at the Brookhaven National Laboratory (BNL) has measured this quantity to be [2]

$$a_\mu^{\text{E821}} = 116592089(63) \times 10^{-11} . \quad (2)$$

This measurement was recently updated by the Muon $g - 2$ experiment at Fermilab, which observed [3]

$$a_\mu^{\text{FNAL}} = 116592040(54) \times 10^{-11} . \quad (3)$$

The combination of these two experimental results yields a measured value of [3]

$$a_\mu^{\text{exp}} = 116592061(41) \times 10^{-11} , \quad (4)$$

which exceeds the SM prediction by

$$\Delta a_\mu := a_\mu^{\text{exp}} - a_\mu^{\text{SM}} = 251(59) \times 10^{-11} , \quad (5)$$

corresponding 4.2σ discrepancy. While this result awaits further scrutiny, if confirmed, it is the first discovery of new physics beyond the SM at directly accessible energies that cannot be decoupled and therefore requires a viable explanation.

There are many such possibilities to explain the muon $g - 2$ result. From an effective field theory point of view, we write new physics contributions to the magnetic moment of the muon as a dimension-five effective operator

$$\mathcal{L} \supset \epsilon \frac{e m_\mu}{16\pi^2 \Lambda^2} \bar{\mu} \sigma^{\mu\nu} \mu F_{\mu\nu} , \quad (6)$$

with $\epsilon = \pm 1$ depending on new physics. This operator contributes to Δa_μ as

$$\Delta a_\mu = \epsilon \frac{e m_\mu^2}{4\pi^2 \Lambda^2} \approx (251 \times 10^{-11}) \times \left(\frac{\epsilon}{+1} \right) \left(\frac{183 \text{ GeV}}{\Lambda} \right)^2 , \quad (7)$$

which indicates that the muon $g - 2$ excess points to new charged particles in the few hundred GeV mass range.

As the scale of this operator is within reach of direct experimental probe, we turn to study-

ing its origin in a renormalizable theory. One notable possibility is in the framework of the well-studied Minimal Supersymmetric Standard Model (MSSM) [4–6]. Given the long-standing puzzle of the identity of dark matter, another possibility that there is a correlation between muon $g-2$ and dark matter states. Along this direction, we consider a class of models known as “Lepton Portal Dark Matter” (LPDM) [7–9], which represents a class of simplified dark matter models with dark matter coupling directly with a mediator and a charged lepton. Depending on the spin of the dark matter state, the dark matter sector contribution to Δa_μ could be either positive or negative. To explain the observed positive value of Δa_μ , one could have the dark matter to be a scalar and the charged mediator to be a fermion, which is the focus of our work. Even for the minimal model presented in Ref. [7], various experimental searches for dark matter together with a theoretical perturbativity requirement have highly constrained the Δa_μ preferred parameter space (see Ref. [10] for updated status). One notable constraint comes from dark matter indirect detection by searching gamma ray lines from the three-body annihilation with an internal bremsstrahlung photon [11, 12]. In this paper, we will show that those indirect constraints can easily be relaxed if the dark matter state X has multiple degrees of freedom n_f . For large n_f , holding the dark matter mass fixed, the required coupling to explain Δa_μ is reduced by a factor of $1/\sqrt{n_f}$ such that the dark matter annihilation cross section is reduced by a factor of $1/n_f^2$. To further suppress various experimental constraints, we will choose the dark matter to be a real scalar that is a fundamental under an S_{n_f} symmetry.

Our paper is organized as follows. In Section 2, we present the LPDM model with particles charged under gauge and global symmetries. In Section 3, we work out the constraints on the model parameter space from various collider searches including the soft lepton searches aiming for degenerate spectra. We then present the formula to explain Δa_μ in this model in Section 4. Section 5 contains the dark matter phenomenology including the thermal abundance in 5.1, direct detection in 5.2 and indirect detection in 5.3. We conclude our paper in Section 6.

2 The Model

We consider the SM plus three right-handed neutrinos that provide a Seesaw mechanism to explain the light neutrino mass. In the lepton sector, we have

$$\mathcal{L} \supset -Y_e \bar{L}_L H e_R - Y_\nu \bar{L}_L \tilde{H} \nu_R - \frac{1}{2} Y_R M_R \nu_R^T \mathcal{C} \nu_R + h.c., \quad (8)$$

with Y_e , Y_ν , and Y_R as 3×3 mass matrices. Here, \mathcal{C} is the charge-conjugation operator and $\tilde{H} = i\sigma_2 H^*$; M_R sets the general scale for the right-handed neutrinos. Treating the Yukawa matrices as spurion fields, the global symmetry in the lepton sector is $SU(3)_{L_L} \times SU(3)_{e_R} \times SU(3)_{\nu_R} \times U(1)_L$, where we only keep tracking the common lepton number symmetry $U(1)_L$. Under the global symmetry, one has

$$Y_e \in (3, \bar{3}, 1)_0, \quad Y_\nu \in (3, 1, \bar{3})_0, \quad Y_R \in (1, 1, \bar{6})_{-2}. \quad (9)$$

To simplify our discussion, we consider a specific structure for $Y_R = y_R \mathbb{I}_3$, which breaks $SU(3)_{\nu_R} \rightarrow SO(3)_{\nu_R}$ as well as $U(1)_L$. With this assumption, the light neutrino mass matrix is

$$M_\nu = -\frac{v^2}{2} Y_\nu (Y_R M_R)^{-1} Y_\nu^T = -\frac{v^2}{2 y_R M_R} Y_\nu Y_\nu^T, \quad (10)$$

with $v = 246$ GeV as the electroweak scale. In the basis of diagonal charged-lepton mass matrix, one has $M_\nu = U_{\text{PMNS}} \hat{m}_\nu U_{\text{PMNS}}^T$ with \hat{m}_ν as the diagonal neutrino mass matrix.

In the dark matter sector, we introduce (real) scalars X^a with $a = 1, \dots, n_f$ as the dark matter flavor index that contains the dark matter candidate and a vector-like charged fermion ψ_L and ψ_R that are $(1, 1)_{-1}$ under the SM gauge group and have the same gauge charge as e_R . There is another global discrete symmetry S_{n_f} associated with the number of species of X^a . Under the flavor symmetry, $SU(3)_{L_L} \times SU(3)_{e_R} \times SU(3)_{\nu_R} \times S_{n_f} \times U(1)_L$, we have

$$X \in (1, 1, 1, n_f)_0, \quad \psi \in (1, 3, 1, 1)_1, \quad (11)$$

and both are \mathcal{Z}_2 -odd under a dark parity. The renormalizable interactions are

$$\begin{aligned} \mathcal{L} &\supset -Y_X^a X^a \overline{\psi_L^i} e_R^i - Y_\psi \mu \overline{\psi_L^i} \psi_R^i + h.c. - \frac{1}{2} M_X^2 X^a X^a \\ &= -\lambda X^a \overline{\psi_L^i} e_R^i - m_\psi \overline{\psi_L^i} \psi_R^i + h.c. - \frac{1}{2} M_X^2 X^a X^a, \end{aligned} \quad (12)$$

with $Y_X^a = \lambda$ for all a to conserve the S_{n_f} symmetry. In our study, we will consider degenerate masses for all n_f X^a or the dark matter candidate X contains a number of degrees of freedom n_f . For the three electrically-charged fermions, ψ^i or $\psi_{e,\mu,\tau}$, we assume that they have an approximately degenerate spectrum, although the flavor symmetry breaking spurion could change the story. For instance, the ψ_τ field that couples to the τ lepton could be slightly heavier than the other two ψ_μ and ψ_e . So, there are totally 5 parameters in our model: $\lambda, M_X, m_\psi, n_f$ and $\Delta m_{\psi_\tau} \equiv m_{\psi_\tau} - m_{\psi_{e,\mu}}$. For most of our studies later, the last parameter Δm_{ψ_τ} does not play a significant role. For the presentation purpose, we also define $\Delta m \equiv m_\psi - M_X$.

To explain Δa_μ , the coupling strength λ is required to be large. So, when we consider the renormalization group equation (RGE) running of λ , we can approximately ignore the SM gauge, Yukawa and quartic couplings. At two-loop level, one has [13]

$$\frac{d\lambda}{d \ln \mu} \equiv \beta_\lambda(\lambda) = 5 n_f \frac{\lambda^3}{(4\pi)^2} - \frac{57}{4} n_f^2 \frac{\lambda^5}{(4\pi)^4}. \quad (13)$$

Note that there exists an ultra-violet (UV) fixed point value λ_* with $\beta(\lambda_*) = 0$ and

$$\lambda_* = \frac{4\pi}{\sqrt{n_f}} \sqrt{\frac{20}{57}} \approx \frac{7.4}{\sqrt{n_f}}. \quad (14)$$

based on the perturbative calculation. For a large coupling λ at the scale of ~ 100 GeV, the

theory could become a strongly coupled one with a nearby Landau-pole scale. The existence of UV fixed point suggests that the UV completion model could have an (approximately) conformal symmetry.

3 The collider constraints

Current collider constraints on this model can be obtained by recasting searches for sleptons at the LHC. In addition to the LHC constraints, m_ψ must be larger than roughly 100 GeV nearly independent of $\Delta m = m_\psi - M_X$ due to constraints from LEP [14–18]. The dominant constraints come from standard (uncompressed) slepton searches at CMS [19] and ATLAS [20], as well as from a compressed slepton search at ATLAS [21]. The latter combines a search for missing energy with tagging soft leptons to reduce the QCD background and achieve good sensitivity to lepton portal models for Δm between around 1 GeV and 40 GeV, effectively closing the gap for the lepton portal down to 1 GeV splitting and up to a few hundred GeV in mass.

To recast these results, we take the combined observed limits on the selectron and smuon cross section in each search and compare with an leading order calculation of the total electron and muon flavor portal mediator cross section using `MadGraph5 2.9.2` [22] with a model implemented in `FeynRules 2.3.41` [23]. These limits are presented by CMS in Figure 14 of Ref. [19], ATLAS in Auxiliary Figure 3a of Ref. [21] for the standard slepton search, and ATLAS in Auxiliary Table 11 of Ref. [20] for the compressed slepton search. The shaded regions in Fig. 2 correspond to cross sections exceeding these limits. One can see that the collider results allow a compressed spectrum with the mass splitting below around 1 GeV or between 40 GeV and 100 GeV for M_X below 300 GeV.

4 Muon anomalous magnetic moment

Loop diagrams with X and ψ can generate a positive contribution to the muon anomalous magnetic moment $a_\mu = (g - 2)_\mu/2$. At one-loop, the new physics contribution from the dark matter sector is

$$\Delta a_\mu^{(X,\psi)} = \frac{n_f \lambda^2 m_\mu^2}{16\pi^2 M_X^2} \left[\frac{2 + 3x - 6x^2 + x^3 + 6x \ln x}{6(1-x)^4} \right], \quad (15)$$

with $x \equiv m_\psi^2/M_X^2$. In the degenerate limit with $x = 1$, the value in the bracket is 1/12. In the opposite limit with $x \rightarrow 0$ or $m_\psi \gg M_X$, one has

$$\Delta a_\mu^{(X,\psi)} \approx \frac{n_f \lambda^2 m_\mu^2}{16\pi^2 m_\psi^2} \frac{1}{6}. \quad (16)$$

Note that the specific combination of $n_f \lambda^2$ affects Δa_μ . In the degenerate limit and to explain the central experimental value of Δa_μ , one needs to have $n_f \lambda^2 \approx 4.3 \times (M_X/100 \text{ GeV})^2$. So, to

have a perturbative control of our calculation, we need to consider a lighter M_X . Even when $M_X = 100$ GeV, additional two-loop calculations for Δa_μ are needed to reduce the errors for theoretical predictions. Based on a naive dimension analysis, the two-loop corrections could have a relative error of $\mathcal{O}[n_f \lambda^2/(16\pi^2)]$.

5 Dark matter phenomenology

5.1 Thermal abundance

Although the dark matter abundance could be explained by some non-thermal early universe, the thermal one and especially the weakly interacting massive particle (WIMP) miracle provides a strong motivation for us to correlate the muon $g - 2$ measurement to dark matter. So, we discuss the potential parameter space to have a thermal dark matter in the lepton-portal dark matter model.

Because X is a real scalar, its self-annihilations to leptons are either helicity suppressed or velocity suppressed. For the leading s -, p - and d -wave ones, the annihilation rate is ¹

$$\sigma v(XX \rightarrow \ell^+ \ell^-) = \frac{\lambda^4 m_\ell^2}{4\pi(M_X^2 + m_\psi^2)^2} - v^2 \frac{\lambda^4 m_\ell^2 M_X^2 (M_X^2 + 2m_\psi^2)}{6\pi (M_X^2 + m_\psi^2)^4} + v^4 \frac{\lambda^4 M_X^6}{60\pi (M_X^2 + m_\psi^2)^4}, \quad (17)$$

where for each term we have kept the leading one in m_ℓ^2/M_X^2 . Because of the helicity suppression for both s and p waves, the dominant contribution to the thermal abundance is the d -wave one. Defining $\sigma_{\text{eff}} v = \sigma v(XX) = s + p v^2 + d v^4$, one has the thermal averaged annihilation rate as $\langle \sigma_{\text{eff}} v \rangle = s + 6 p x^{-1} + 60 d x^{-2}$ with $x \equiv M_X/T$. The freeze-out temperature x_F is given by

$$x_F = \ln \left[\frac{5}{4} \sqrt{\frac{45}{8}} \frac{g}{2\pi^3} \frac{M_{\text{pl}} M_X (s + 6 p x_F^{-1} + 60 d x_F^{-2})}{\sqrt{g^*} \sqrt{x_F}} \right], \quad (18)$$

with $g = n_f$ as the number of degrees of freedom for dark matter. Here, $M_{\text{pl}} = 1.22 \times 10^{19}$ GeV and g^* is the number of relativistic degrees of freedom at T_F and is taken to be 86.25. The dark matter abundance approximately depends on s , p and d as

$$\Omega_X h^2 \approx \frac{1.07 \times 10^9}{\text{GeV} M_{\text{pl}} \sqrt{g^*}} \frac{x_F}{s + 3 p x_F^{-1} + 20 d x_F^{-2}}. \quad (19)$$

If only one wave dominates, one has $s \approx 0.9 \text{ pb} \cdot \text{c}$, $p \approx 7 \text{ pb} \cdot \text{c}$ and $d \approx 27 \text{ pb} \cdot \text{c}$ to satisfy the observed dark matter abundance. Using (17), one has

$$d = \frac{\lambda^4 M_X^6}{60\pi (M_X^2 + m_\psi^2)^4} = (27 \text{ pb} \cdot \text{c}) \times \left(\frac{\lambda}{3}\right)^4 \left(\frac{100 \text{ GeV}}{M_X}\right)^2 \left(\frac{2}{1 + x/4}\right)^4, \quad (20)$$

¹We use the program `Calchep` [24] to calculate some of our formulas.

with $x \equiv m_\psi^2/M_X^2$. One needs to have a large coupling λ to satisfy the thermal dark matter relic abundance. Otherwise, one may worry about the X abundance is too large and overcloses the universe. We have checked that just using the d -wave XX self-annihilation cross section, it is not possible to obtain a thermal dark matter to be consistent with other constraints. On the other hand, additional particles or interactions could be used to make X a thermal dark matter candidate. For instance, one could add an additional Higgs portal coupling to XX to increase the annihilation cross section.

In the parameter region with an approximately degenerate X and ψ with $\Delta m/M_X \lesssim 1/25$, the coannihilations of dark matter states can provide another interesting thermal dark matter parameter space. Here, we list the formulas for the dominant annihilation processes that have a nonzero s -wave annihilation rate. The annihilation rates for $X_a\psi_i^-$ have

$$\sigma v(X_a\psi_i^- \rightarrow \ell_i^- \gamma) = \frac{e^2 \lambda^2}{32\pi M_X (M_X + m_\psi)}, \quad \sigma v(X_a\psi_i^- \rightarrow \ell_i^- Z) = \frac{e^2 \lambda^2 s_W^2 [(M_X + m_\psi)^2 - M_Z^2]^2}{32\pi c_W^2 M_X (M_X + m_\psi)^5}.$$

The flavor-specific two-lepton annihilation rate for $\psi_i^- \psi_i^+$ mediated by X particles is

$$\sigma v(\psi_i^- \psi_i^+ \rightarrow \ell_i^- \ell_i^+) = \frac{n_f \lambda^4 m_\psi^2}{32\pi (M_X^2 + m_\psi^2)^2}. \quad (21)$$

Mediated by photon and the Z boson, one flavor of $\psi_i^- \psi_i^+$ can also annihilate into all three charged leptons. The rate is given by

$$\sigma v(\psi_i^- \psi_i^+ \rightarrow \gamma^*/Z \rightarrow \ell^- \ell^+) = \frac{3 e^4 (M_W^4 - 6M_W^2 m_\psi^2 + 10m_\psi^4)}{16\pi m_\psi^2 (M_W^2 - 4c_W^2 m_\psi^2)^2}, \quad (22)$$

with the overall factor of 3 from counting three charged leptons. Similarly, the annihilation rates to quarks are

$$\begin{aligned} \sigma v(\psi_i^- \psi_i^+ \rightarrow \gamma^*/Z \rightarrow d\bar{d}, s\bar{s}, b\bar{b}) &= \frac{3 e^4 (M_W^4 - 2M_W^2 m_\psi^2 + 10m_\psi^4)}{48\pi m_\psi^2 (M_W^2 - 4c_W^2 m_\psi^2)^2}, \\ \sigma v(\psi_i^- \psi_i^+ \rightarrow \gamma^*/Z \rightarrow u\bar{u}, c\bar{c}) &= \frac{2 e^4 (2M_W^4 - 10M_W^2 m_\psi^2 + 17m_\psi^4)}{24\pi m_\psi^2 (M_W^2 - 4c_W^2 m_\psi^2)^2}. \end{aligned} \quad (23)$$

The annihilation rates to gauge bosons are given by

$$\begin{aligned} \sigma v(\psi_i^- \psi_i^+ \rightarrow \gamma\gamma) &= \frac{e^4}{16\pi m_\psi^2}, \\ \sigma v(\psi_i^- \psi_i^+ \rightarrow ZZ) &= \frac{e^4 s_W^4 (c_W^2 m_\psi^2 - M_W^2)^{3/2}}{4\pi c_W^3 m_\psi (M_W^2 - 2c_W^2 m_\psi^2)^2}, \quad \sigma v(\psi_i^- \psi_i^+ \rightarrow \gamma Z) = \frac{e^4 s_W^2 (4c_W^2 m_\psi^2 - M_W^2)}{32\pi c_W^4 m_\psi^4}, \\ \sigma v(\psi_i^- \psi_i^+ \rightarrow W^- W^+) &= \frac{e^4 (4m_\psi^6 + 16m_\psi^4 M_W^2 - 17m_\psi^2 M_W^4 - 3M_W^6)}{64\pi m_\psi^4 (M_W^2 - 2c_W^2 m_\psi^2)^2} \sqrt{1 - \frac{M_W^2}{m_\psi^2}}, \end{aligned} \quad (24)$$

Finally, the annihilation rate to Zh is given by

$$\begin{aligned} \sigma v(\psi_i^- \psi_i^+ \rightarrow Zh) &= \frac{e^4 [16m_\psi^4 - 8m_\psi^2(M_h^2 - 5M_Z^2) + (M_h^2 - M_Z^2)^2]}{1024\pi c_W^4 m_\psi^4 (M_Z^2 - 4m_\psi^2)^2} \\ &\quad \times \sqrt{M_h^4 - 2M_h^2(4m_\psi^2 + M_Z^2) + (M_Z^2 - 4m_\psi^2)^2} . \end{aligned} \quad (25)$$

In the very degenerate coannihilation region with $\Delta m/M_X \ll x_F$, the effective annihilation rate is given by [25]

$$\sigma_{\text{eff}} v = \sigma_{ij} \frac{g_i g_j}{g_{\text{eff}}^2} = \frac{24}{g_{\text{eff}}^2} [\sigma v(\psi_i^- \psi_i^+) + n_f \sigma v(X_a \psi_i^-)] , \quad (26)$$

by ignoring the small annihilation rate of $\sigma v(XX)$. Here, the total degrees of freedom is $g_{\text{eff}} = 12 + n_f$ by including both 3 ψ 's and n_f X 's.

5.2 Direct detection

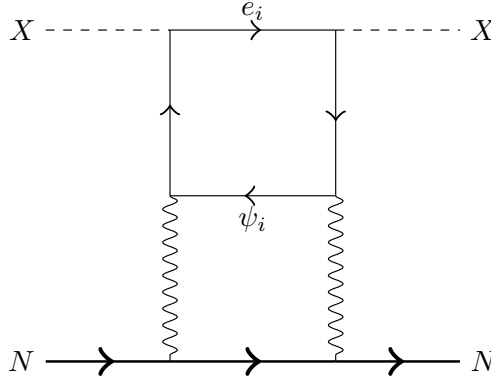


Figure 1: Sample diagram for the dark matter candidate scattering off a nucleus at two-loop level. There are several other diagrams corresponding to crossings and interchanging charged-particles.

The dark matter scalar X does not have any interactions with hadrons at tree level. At loop level, it couples via photons. For a real scalar X , there is no one-photon coupling, so the leading interaction occurs at two loops and involves the exchange of two photons. A diagram for scattering off a nucleus including an effective two photon operator is shown in Fig. 1. Integrating out the upper box loop in Fig. 1, one has the resulting two photon coupling operator as

$$\mathcal{L} \supset -C_1 \frac{\lambda^2 \alpha}{4 \pi m_\psi^2} X^2 F_{\mu\nu} F^{\mu\nu} , \quad (27)$$

with $C_1 = \mathcal{O}(1)$. This operator generates a coupling to nuclei via the two-photon form factor. Such a coupling has been studied in Ref. [26], where it was found that the dark matter-nucleus

cross section is given by

$$\sigma_{XN} \approx \frac{144\pi}{25} \mu_{XN}^2 Z^4 \alpha^2 \frac{\chi_E^2}{r_0^2}, \quad (28)$$

where μ_{XN} is the reduced mass of the χ - N , Z is the atomic number of the nucleus, r_0 is the charge radius of the nucleus $r_0 \sim 1.2 \text{ fm } A^{1/3}$, and χ_E is the coupling of dark matter to \mathbf{E}^2 . The latter coefficient is related to the two-photon operator by

$$\chi_E \sim \frac{\lambda^2 \alpha}{4\pi m_\psi^2 M_X}. \quad (29)$$

Spin-independent direct detection constraints are typically presented as the cross section for scattering off a nucleon, which is related to the cross section for scattering off a nucleus by

$$\sigma_{Xn} = \sigma_{XN} \frac{m_n^2}{\mu_{XN}^2 A^2}, \quad (30)$$

so that we find for Xenon

$$\sigma_{Xn} \sim (2 \times 10^{-49} \text{ cm}^2) \left(\frac{\lambda}{2.5}\right)^4 \left(\frac{150 \text{ GeV}}{M_X}\right)^2 \left(\frac{150 \text{ GeV}}{m_\psi}\right)^4, \quad (31)$$

which remains out of the reach of current Xenon-based direct detection experiments [27].

The scattering cross section of X with a non-relativistic electron can happen at tree-level and is given by

$$\sigma(Xe^- \rightarrow Xe^-) = \frac{\lambda^4 m_e^4 (M_X^2 + m_\psi^2)^2}{4\pi M_X^2 (m_\psi^2 - M_X^2)^4} = (9 \times 10^{-46} \text{ cm}^2) \left(\frac{\lambda}{2.5}\right)^4 \left(\frac{150 \text{ GeV}}{M_X}\right)^2 \left(\frac{1 \text{ GeV}}{\Delta m}\right)^4 \quad (32)$$

Due to the additional m_e^2 suppression of this cross section, this interaction too remains out the reach of current direct detection experiments, which constraint this cross section at the 10^{-38} cm^2 level at $M_X \approx 100 \text{ GeV}$ [28].

5.3 Indirect detection

The dominant constraint on the lepton portal from indirect detection comes from searches for the peaked tail of internal bremsstrahlung photon production. This process produces a photon with a sharp peak just below the maximum photon energy. We calculate the internal bremsstrahlung cross section and compare with the limits on σv obtained in Ref. [12] using Fermi-LAT galactic center photon data. The internal bremsstrahlung cross section is given by

$$\langle\sigma v\rangle_{\text{IB}} = \frac{\alpha \lambda^4}{8\pi^2 M_X^2} F(m_\psi^2/M_X^2), \quad (33)$$

with

$$F(\mu) = (1 + \mu) \left[\frac{\pi^2}{6} - \log^2 \frac{1 + \mu}{2\mu} - 2 \text{Li}_2 \left(\frac{1 + \mu}{2\mu} \right) \right] + \frac{4\mu + 3}{\mu + 1} + \frac{(4\mu + 1)(\mu - 1)}{2\mu} \log \frac{\mu - 1}{\mu + 1}. \quad (34)$$

Note that in $F(1) \rightarrow 7/2 - \pi^2/3$ and $F(\infty) \rightarrow 4/(15\mu^4)$. Our calculation of the cross section agrees with that of Ref. [10]. Since this is a line search, it has reduced dependence on astrophysical backgrounds that generally do not yield line-like signatures. Note, however, that these results are subject to uncertainty based on the profile of dark matter in the galactic center, as more peaked profiles lead to regions with enhanced squared density. Profiles including Einasto [29], Navarro-Frenk-White (NFW) [30], and isothermal vary by as much as a factor of 3 in their projected limits [31]. For a fixed dark matter mass, as we increase the internal degrees of freedom of dark matter n_f , the required coupling λ to explain Δa_μ is reduced by a factor of $1/\sqrt{n_f}$. As a result, the indirect detection limit is relaxed by a factor of n_f^2 . Therefore, we will choose $n_f = 30$ as a representative one to relax the constraints from indirect detection.

6 Discussion and conclusions

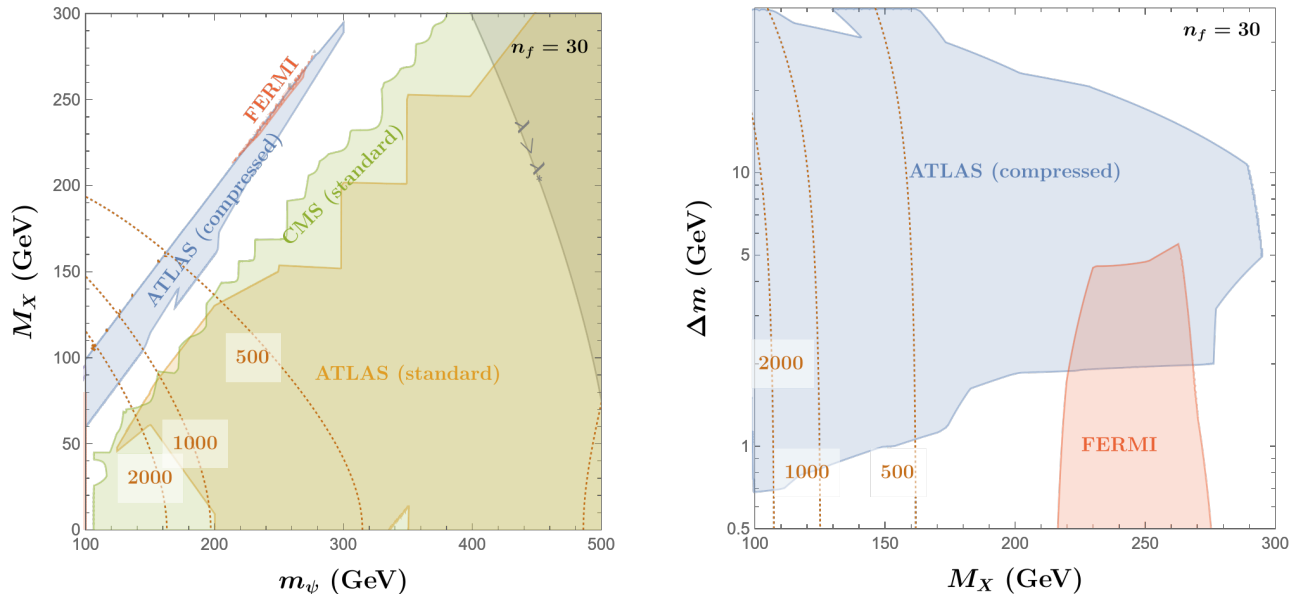


Figure 2: Constraints on the LPDM from collider, indirect detection, and perturbativity after fixing the coupling λ to match the central value of the observed Δa_μ and taking $n_f = 30$. The dashed lines indicate the scale in GeV of the Landau pole at which the theory becomes strongly coupled. The left panel shows a broad parameter space, while the right panel focuses on the compressed region.

The results of our study are summarized in Fig. 2. In both panels, we fix λ to fit the central value of the observed Δa_μ . Various constraints from collider and indirect detection as discussed

in detail above are shown in the shaded regions. We assume that there are $n_f = 30$ species of dark matter X . The shaded gray region indicates the parameter space where the λ required to fit Δa_μ is naively greater than λ_* of the UV fixed point. In this region, perturbation theory can certainly not be trusted and higher order corrections will be very important. In addition, due to the relatively large couplings required to fit the observed Δa_μ , there will be a nearby Landau pole at which the theory becomes strongly coupled, possibly hitting a conformal fixed point of the β function. The scale at which the one-loop running $\lambda(\Lambda) = \lambda_*$ is indicated by the dashed lines for 500 GeV, 1 TeV and 2 TeV, indicating a Landau pole. The left panel indicates that a Δm between roughly 40 GeV and 100 GeV may be accommodated, while the right panel indicates that a Δm below 1 GeV may be allowed.

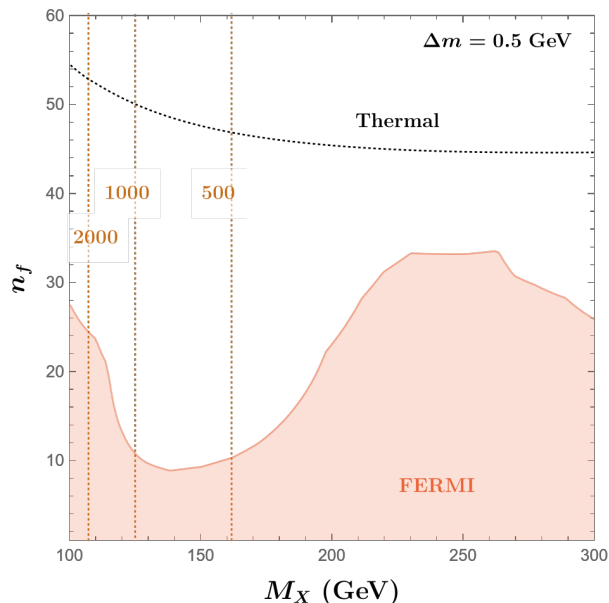


Figure 3: The dark matter mass and n_f for which the model predicts the observed relic abundance of dark matter through co-annihilation. Constraints from Fermi-LAT gamma ray data are also shown in the shaded region, along with the scale of the Landau pole in GeV in the vertical dashed lines.

It is possible to match the observed abundance of dark matter in a thermal co-annihilating scenario with large n_f between 45 and 55, with larger n_f preferred in order to maximize the scale of the Landau pole. This behavior is illustrated in Fig. 3. The Fermi-LAT result requires n_f to be larger than around 10, though these constraints are subject to astrophysical uncertainties.

If such a nearly degenerate scenario is considered, the ψ_τ is naively stable on collider length scales, as its decay proceeds via an off-shell τ lepton into a four-body final state. Searches for heavy stable charged particles [32, 33] at the LHC rule out this possibility. It is possible, however, to moderately split the ψ_τ from the ψ_e and ψ_μ in a minimal flavor violating (MFV) [34] scenario, where the non-degenerate correction to the ψ_i mass is proportional to $Y_{e,i}^\dagger Y_{e,i}$. Only a small splitting such that $m_\psi - M_X > m_\tau$ is required. The LPDM scenario here bears some resemblance to Flavored Dark Matter [9, 35]. The flavor structure we consider is simpler in order

to avoid constraints from signals like $\mu \rightarrow e\gamma$ decay as our focus is on offering an explanation of the Muon $g - 2$ result.

In summary, we have found that there exists allowed parameter space in LPDM that explains the Δa_μ excess. The dark matter states including the charged states ψ_i must be below a few hundred GeV. Future experiments can further probe this scenario. At colliders, the high luminosity LHC can improve on the compressed spectrum searches with soft leptons in the final state. A future lepton collider with $\sqrt{s} \gtrsim 500$ GeV would nearly completely probe the allowed region. Future gamma ray line searches at Cherenkov Telescope Array [36] and GAMMA-400 [37] can also potentially discover the dark matter candidates.

Acknowledgements

The work of YB is supported by the U. S. Department of Energy under the contract DE-SC0017647. The work of JB is supported by start up funds from Colorado State University.

References

- [1] T. Aoyama et al., *The anomalous magnetic moment of the muon in the Standard Model*, *Phys. Rept.* **887** (2020) 1–166, [[arXiv:2006.04822](#)].
- [2] **Muon g-2** Collaboration, G. W. Bennett et al., *Final Report of the Muon E821 Anomalous Magnetic Moment Measurement at BNL*, *Phys. Rev. D* **73** (2006) 072003, [[hep-ex/0602035](#)].
- [3] **Muon g - 2** Collaboration, B. Abi et al., *Measurement of the positive muon anomalous magnetic moment to 0.46 ppm*, *Phys. Rev. Lett.* **126** (Apr, 2021) 141801.
- [4] D. J. H. Chung, L. L. Everett, G. L. Kane, S. F. King, J. D. Lykken, and L.-T. Wang, *The Soft supersymmetry breaking Lagrangian: Theory and applications*, *Phys. Rept.* **407** (2005) 1–203, [[hep-ph/0312378](#)].
- [5] T. Moroi, *The Muon anomalous magnetic dipole moment in the minimal supersymmetric standard model*, *Phys. Rev. D* **53** (1996) 6565–6575, [[hep-ph/9512396](#)]. [Erratum: *Phys.Rev.D* **56**, 4424 (1997)].
- [6] S. P. Martin and J. D. Wells, *Muon Anomalous Magnetic Dipole Moment in Supersymmetric Theories*, *Phys. Rev. D* **64** (2001) 035003, [[hep-ph/0103067](#)].
- [7] Y. Bai and J. Berger, *Lepton Portal Dark Matter*, *JHEP* **08** (2014) 153, [[arXiv:1402.6696](#)].
- [8] S. Chang, R. Edezhath, J. Hutchinson, and M. Luty, *Leptophilic Effective WIMPs*, *Phys. Rev. D* **90** (2014), no. 1 015011, [[arXiv:1402.7358](#)].
- [9] P. Agrawal, Z. Chacko, and C. B. Verhaaren, *Leptophilic Dark Matter and the Anomalous Magnetic Moment of the Muon*, *JHEP* **08** (2014) 147, [[arXiv:1402.7369](#)].

- [10] J. Kawamura, S. Okawa, and Y. Omura, *Current status and muon $g - 2$ explanation of lepton portal dark matter*, *JHEP* **08** (2020) 042, [[arXiv:2002.12534](#)].
- [11] **Fermi-LAT** Collaboration, M. Ackermann et al., *Search for Gamma-ray Spectral Lines with the Fermi Large Area Telescope and Dark Matter Implications*, *Phys. Rev. D* **88** (2013) 082002, [[arXiv:1305.5597](#)].
- [12] M. Garny, A. Ibarra, M. Pato, and S. Vogl, *Internal bremsstrahlung signatures in light of direct dark matter searches*, *JCAP* **12** (2013) 046, [[arXiv:1306.6342](#)].
- [13] F. Staub, *SARAH 4 : A tool for (not only SUSY) model builders*, *Comput. Phys. Commun.* **185** (2014) 1773–1790, [[arXiv:1309.7223](#)].
- [14] **ALEPH** Collaboration, A. Heister et al., *Search for scalar leptons in $e^+ e^-$ collisions at center-of-mass energies up to 209-GeV*, *Phys. Lett. B* **526** (2002) 206–220, [[hep-ex/0112011](#)].
- [15] **ALEPH** Collaboration, A. Heister et al., *Absolute mass lower limit for the lightest neutralino of the MSSM from $e^+ e^-$ data at $s^{**}(1/2)$ up to 209-GeV*, *Phys. Lett. B* **583** (2004) 247–263.
- [16] **DELPHI** Collaboration, J. Abdallah et al., *Searches for supersymmetric particles in $e^+ e^-$ collisions up to 208-GeV and interpretation of the results within the MSSM*, *Eur. Phys. J. C* **31** (2003) 421–479, [[hep-ex/0311019](#)].
- [17] **L3** Collaboration, P. Achard et al., *Search for scalar leptons and scalar quarks at LEP*, *Phys. Lett. B* **580** (2004) 37–49, [[hep-ex/0310007](#)].
- [18] **OPAL** Collaboration, G. Abbiendi et al., *Search for anomalous production of dilepton events with missing transverse momentum in $e^+ e^-$ collisions at $s^{**}(1/2) = 183$ -GeV to 209-GeV*, *Eur. Phys. J. C* **32** (2004) 453–473, [[hep-ex/0309014](#)].
- [19] **CMS** Collaboration, A. M. Sirunyan et al., *Search for supersymmetry in final states with two oppositely charged same-flavor leptons and missing transverse momentum in proton-proton collisions at $\sqrt{s} = 13$ TeV*, [arXiv:2012.08600](#).
- [20] **ATLAS** Collaboration, G. Aad et al., *Search for electroweak production of charginos and sleptons decaying into final states with two leptons and missing transverse momentum in $\sqrt{s} = 13$ TeV pp collisions using the ATLAS detector*, *Eur. Phys. J. C* **80** (2020), no. 2 123, [[arXiv:1908.08215](#)].
- [21] **ATLAS** Collaboration, G. Aad et al., *Searches for electroweak production of supersymmetric particles with compressed mass spectra in $\sqrt{s} = 13$ TeV pp collisions with the ATLAS detector*, *Phys. Rev. D* **101** (2020), no. 5 052005, [[arXiv:1911.12606](#)].
- [22] J. Alwall, M. Herquet, F. Maltoni, O. Mattelaer, and T. Stelzer, *MadGraph 5 : Going Beyond*, *JHEP* **06** (2011) 128, [[arXiv:1106.0522](#)].
- [23] A. Alloul, N. D. Christensen, C. Degrande, C. Duhr, and B. Fuks, *FeynRules 2.0 - A complete toolbox for tree-level phenomenology*, *Comput. Phys. Commun.* **185** (2014) 2250–2300, [[arXiv:1310.1921](#)].

- [24] A. Pukhov, *CalcHEP 2.3: MSSM, structure functions, event generation, batchs, and generation of matrix elements for other packages*, [hep-ph/0412191](#).
- [25] K. Griest and D. Seckel, *Three exceptions in the calculation of relic abundances*, *Phys. Rev. D* **43** (1991) 3191–3203.
- [26] M. Pospelov and T. ter Veldhuis, *Direct and indirect limits on the electromagnetic form-factors of WIMPs*, *Phys. Lett. B* **480** (2000) 181–186, [[hep-ph/0003010](#)].
- [27] **XENON** Collaboration, E. Aprile et al., *Dark Matter Search Results from a One Ton-Year Exposure of XENON1T*, *Phys. Rev. Lett.* **121** (2018), no. 11 111302, [[arXiv:1805.12562](#)].
- [28] **XENON** Collaboration, E. Aprile et al., *Light Dark Matter Search with Ionization Signals in XENON1T*, *Phys. Rev. Lett.* **123** (2019), no. 25 251801, [[arXiv:1907.11485](#)].
- [29] S. A. Kutuzov and J. Einasto, *On constructing models of stellar systems. I. On the classification of the models.*, *Publications of the Tartu Astrofizica Observatory* **36** (Jan., 1968) 341–356.
- [30] J. F. Navarro, C. S. Frenk, and S. D. M. White, *A Universal density profile from hierarchical clustering*, *Astrophys. J.* **490** (1997) 493–508, [[astro-ph/9611107](#)].
- [31] **Fermi-LAT** Collaboration, M. Ackermann et al., *Fermi LAT Search for Dark Matter in Gamma-ray Lines and the Inclusive Photon Spectrum*, *Phys. Rev. D* **86** (2012) 022002, [[arXiv:1205.2739](#)].
- [32] **CMS** Collaboration, S. Chatrchyan et al., *Searches for Long-Lived Charged Particles in pp Collisions at $\sqrt{s}=7$ and 8 TeV*, *JHEP* **07** (2013) 122, [[arXiv:1305.0491](#)].
- [33] **ATLAS** Collaboration, G. Aad et al., *Searches for heavy long-lived charged particles with the ATLAS detector in proton-proton collisions at $\sqrt{s} = 8$ TeV*, *JHEP* **01** (2015) 068, [[arXiv:1411.6795](#)].
- [34] C.-J. Lee and J. Tandean, *Lepton-Flavored Scalar Dark Matter with Minimal Flavor Violation*, *JHEP* **04** (2015) 174, [[arXiv:1410.6803](#)].
- [35] P. Agrawal, S. Blanchet, Z. Chacko, and C. Kilic, *Flavored Dark Matter, and Its Implications for Direct Detection and Colliders*, *Phys. Rev. D* **86** (2012) 055002, [[arXiv:1109.3516](#)].
- [36] M. Actis, G. Agnetta, F. Aharonian, A. Akhperjanian, J. Aleksić, E. Aliu, D. Allan, I. Allekotte, F. Antico, and et al., *Design concepts for the cherenkov telescope array cta: an advanced facility for ground-based high-energy gamma-ray astronomy*, *Experimental Astronomy* **32** (Nov, 2011) 193–316.
- [37] A. Galper, O. Adriani, R. Aptekar, I. Arkhangelskaja, A. Arkhangelskiy, M. Boezio, V. Bonvicini, K. Boyarchuk, Y. Gusakov, M. Farber, and et al., *Status of the gamma-400 project*, *Advances in Space Research* **51** (Jan, 2013) 297–300.